Batch and fixed-bed adsorption of tartrazine azo-dye onto activated carbon prepared from apricot stones

H. I. Albroomi[1] · M. A. Elsayed[2] · A. Baraka[2] · M. A. Abdelmaged[2]

Abstract This work describes the potential of utilizing prepared activated carbon from apricot stones as an efficient adsorbent material for tartrazine (TZ) azo-dye removal in a batch and dynamic adsorption system. The results revealed that activated carbons with well-developed surface area (774 m^2/g) and pore volume (1.26 cm^3/g) can be manufactured from apricot stones by H_3PO_4 activation. In batch experiments, effects of the parameters such as initial dye concentration and temperature on the removal of the dye were studied. Equilibrium was achieved in 120 min. Adsorption capacity was found to be dependent on the initial concentration of dye solution, and maximum adsorption was found to be 76 mg/g at 100 mg/L of TZ. The adsorption capacity at equilibrium (q_e) increased from 22.6 to 76 mg/g with an increase in the initial dye concentrations from 25 to 100 mg/L. The thermodynamic parameters such as change in free energy (ΔG^0), enthalpy (ΔH^0) and entropy (ΔS^0) were determined and the positive value of (ΔH) 78.1 (K J mol^{-1}) revealed that adsorption efficiency increased with an increase in the process temperature. In fixed-bed column experiments, the effect of selected operating parameters such as bed depth, flow rate and initial dye concentration on the adsorption capacity was evaluated. Increase in bed height of adsorption columns leads to an extension of breakthrough point as well as the exhaustion time of adsorbent. However, the maximum adsorption capacities decrease with increases of flow rate. The breakthrough data fitted well to bed depth service time and Thomas models with high coefficient of determination, $R^2 \geq 94$.

Introduction

Azo-dyes as an aromatic molecular structure compound are generally resistant to light, biodegradation, temperature, ozonation and oxidation. This significant properties makes the dyes to be accumulated in the living organisms and therefore leading to severe diseases and function disorders (Gautam et al. 2015b). The issue of the presence of color in effluent has received considerable critical attention for dyestuff manufacturers and textile companies (Annadurai et al. 2002). This is because increasingly stringent water quality standards which have been used to controlling and reducing discharge of hazardous substances in effluent (Yavuz and Aydin 2006; Santhy and Selvapathy 2006). Nowadays, there is a primary concern of decolorization and treatment of wastewater because many industries depend on dyes to color their products such as textiles, leather and food processing industries (Robinson et al. 2001). There are various physical and chemical treatment processes for organic dyes removals from wastewater have been applied. The most important treatment processes are coagulation and flocculation, photo-degradation, biosorption, oxidizing agents, membrane and ultra-filtration. The advantages, disadvantages and limitations of each technique have been extensively studied by many researchers (Namasivayam and Suba 2001; Robinson et al. 2001; Gurses et al. 2004; Klán and Vavrik 2006). Due to many draw-backs such as, complexity of the process, low removal efficiencies and

✉ M. A. Elsayed
aboelfotoh@gmail.com

[1] Oman Armed Forces, Masqat, Oman

[2] Chemical Engineering Department, Military Technical College, Egyptian Armed Forces, Cairo, Egypt

relatively high operating costs using the above-mentioned techniques, dyestuff manufacturers and paper industries seldom apply these methods to treat their wastewater effluents (Robinson et al. 2002; Kadirvelu et al. 2003). However, regarding to initial operating costs, ease of operation, simplicity of equipments design, adsorption onto activated carbon process has been found to be an efficient and economic process to remove dyes and other pollutant from wastewater (Annadurai and Lee 2002; Grégorio Crini 2010; Algidsawi 2011).

Although batch adsorption studies provide useful data and parameters on the application of specific adsorbents for the removal of dyes or specific pollutant, continuously fixed bed or column experiments are also necessary to provide practical operational information with respect to the adsorption of constituents with the use of a particular adsorbent (Ahmad and Hameed 2010; Dutta and Basu 2014). Fixed-bed columns can be operated singly, in series or in parallel. Small-scale column tests can be employed to simulate the potential performance of the adsorbent and the results obtained extrapolated in the design of full-scale reactors (Walker and Weatherley 1997; Futalan et al. 2011; Mulgundmath et al. 2012).

Tartrazine is a synthetic lemon yellow azo-dye authorized in many countries in food processing manufacture with maximum permitted use levels of 50–500 mg/kg-food for various food processing. It is also known as E number E102, C.I. 19140, FD&C Yellow 5, Acid Yellow 23, and Food Yellow 4. Reduction of Tartrazine may produce sulphonated aromatic amines compounds, which have low toxicity potential (Aguilar et al. 2009). Tartrazine is considered to be toxic to humans as it acts as hyperactivity and causes asthma, migraines, eczema, thyroid cancer and other behavioral problems (Gautam et al. 2015a).
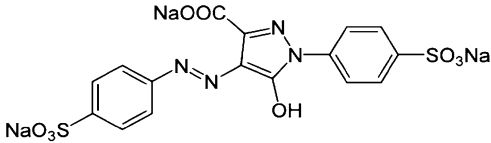
On the basis of the previous discussions, the focus of this research was to evaluate the adsorption potential of the Apricot stone-based activated carbon in removing Tartrazine azo-dye from aqueous solutions through batch and fixed-bed experiments. Batch adsorption experiments were conducted using synthetic aqueous solutions of tartrazine and the effects of initial dye concentration and temperature were investigated. Thermodynamics of the adsorption process has also been studied and the changes in Gibbs free energy, enthalpy and the entropy have been determined. In column experiments, effects of parameters such as flow rate, initial concentration of TZ, and fixed-bed height on TZ adsorption using; Thomas, bed depth service time (BDST) and Adams–Bohart kinetic models were considered.

Experimental

Materials and apparatus

Tartrazine dye supplied by Morgan Chemical Company was used without further purification to prepare all synthetic wastewater solutions. It was kept in a tightly sealed bottle to prevent any contaminations and assure the material quality. Other reagents include phosphoric acid (H_3PO_4), dilute HCl and NaOH solutions. All reagents were of analytical grade. Deionized water was used throughout the experiments. The dyes concentrations were determined using Agilant UV–Vis Cary 60 PC scan double beam recording spectrophotometer using (1) cm glass cells. The measurement of Tartrazine concentration was conducted at $\lambda_{max} = 425$ nm. A digital pH meter, type 720 WTW 82362 was used to adjust the pH. Schematic structure of Tartrazine and its properties are shown in Table 1.

Table 1 Schematic structure of Tartrazine and its properties

Properties	
Chemical structure	
Chemical name	Trisodium (4E)-5-oxo-1-(4-sulfonatophenyl)-4-[(4-sulfonatophenyl)hydrazono]-3-pyrazolecarboxylate
Molecular formula	$C_{16}H_9N_4Na_3O_9S_2$
Molecular weight (g/mol)	534.3 g/mol
Tartrazine purity (%)	≥98 %
Maximum wavelength λ (nm)	427 ± 2 nm
Solubility	Soluble in cold water, hot water

Adsorbent preparation

In this study, activated carbon was prepared from apricot stones by chemical activation technique using phosphoric acid (H_3PO_4) as activating agent. Chemical activation is known by its advantage compared to physical activation in crosslinking and protective of carbon skeleton and its participation in the creation and expansion of the pores (Deng et al. 2009). In addition, chemical activation using phosphoric acid is known to prevent excessive sample burn-off, resulting in high yield and well-developed internal porosity. Firstly, the apricot stones were dried at room temperature then crushed with a jaw crusher. The resulting particles were sieved and the particles having sizes between 1–2 mm were used in the rest of the experimental work. Then samples were treated with the 50 % (vol) H_3PO_4 solution at 25 °C at ratio of 2.5:1 (weight) for 24 h.

After impregnation, solution was filtered to take the residual acid. Subsequently impregnated samples were air dried at room temperature for 3 days. Impregnated apricot stones samples containing %18 H_3PO_4 were obtained after drying. To produce activated carbon, acid impregnated samples were heated; at a heating rate of 20 °C/min to the final carbonization temperatures, 700 °C, for 180 min. Before the characterization, products were crushed to obtain small particles (30–70 mesh or 0.595–0.212 mm) and rinsed with boiling distilled water to decrease the pH value of the activated carbon.

Physicochemical characterization of the adsorbent

BET surface area and micropore volume of each activated carbon were determined from the N_2 adsorption experiments. Approximately 0.12 g samples were heated to 250 °C to remove all the adsorbed species. Nitrogen adsorption and desorption isotherms were then taken using Quantrachrome Autosorb I-CLP Surface Area Analyzer (Micromeritics Instrument Corp.). According to the resulting isotherm, the BET surface area (S_{BET}), micropore volume (V_{mic}), micropore surface area (S_{mic}), mesopore volume (V_{BJH}), mesopore surface area (S_{BJH}), and pore size of the samples were analyzed by BET (Brunauere Emmette Teller) theory, t-plot theory and BJH (Barrette Johnere Halendar) theory, respectively.

For the chemical characterization, the analyses were limited to determination of C, H, N, O elements, ash analysis and FTIR; to provide information with respect to elemental composition and functional groups, respectively. The proximate analysis of the prepared activated carbon was performed according to ASTM standards (Aygun et al. 2003). A carbon/hydrogen/oxygen/nitrogen/sulfur (C/H/O/N/S) content of activated carbon used in this experimental work was analyzed by elemental analyzer (model CHNO-RAPID, Heraeus Co., Germany). Table 2 shows the proximate and elemental analyses of the prepared activated carbon from apricot stones.

Perkin Elmer Spectrum Infrared Spectrometer with resolution of 4 cm^{-1} in the range of 4000–500 cm^{-1} was used for the FTIR analysis of prepared active carbon. The adsorbent and potassium bromide (KBr) were dried in an oven and then ground together in a ratio of 20:1 (KBr:AC) for FTIR measurement using disk sample method (Gupta et al. 2011).

Batch equilibrium studies

Adsorption tests were performed in a set of Erlenmeyer flasks (250 mL) where 100 mL of TZ solutions with initial concentrations of 25–100 mg/L were placed in these flasks. Equal mass of 0.1 g of the prepared activated carbon with the particle size of 0.595–0.212 mm was added to each flask and kept in an isothermal shaker of 100 rpm at 25 °C to reach equilibrium. The pH of the solutions was natural (pH 6.5). Aqueous samples were taken from the solution and the concentrations were analyzed. All samples were filtered prior to the analysis to minimize the interference of the carbon fines with the analysis. The concentrations of TZ in the supernatant solution before and after adsorption were determined using Agilent UV–Vis Cary 60 PC scan double beam recording spectrophotometer using (1) cm glass cells. Each experiment was duplicated under identical conditions. The amount of adsorption at equilibrium, q_e (mg/g), was calculated by:

$$q_e = \frac{V}{W}(C_0 - C_e) \tag{1}$$

where C_0 and C_e (mg/L) are the liquid phase concentrations of dye at the initial and equilibrium conditions, respectively. V is the volume of the solution (l) and W is the mass of dry adsorbent used (g).

Table 2 Proximate and elemental analyses of prepared active carbon

Sample	Proximate analysis (wt%)			Elemental analysis (wt%)				
	Moisture	Ash	Volatile matter	C	H	N	S	O by diff.
AC	5.1	3.36	82.8	83.12	3.87	0.91	0.56	11.54

Fixed-bed adsorption experiment

The experiment was conducted in a 2 cm diameter and 15 cm length encased Pyrex glass tube having an embedded stainless steel mesh for supporting layer of adsorbent. A schematic of the experimental setup used for column study is shown in Fig. 1. The experiments were conducted by varying the weight of activated carbon and different initial solutions concentration of TZ. The height of the activated carbon bed was measured before the tests to monitor the variation cause by bed height. The Activated carbon 5.6, 7 and 8.4 g adsorbent corresponding to 8, 10 and 12 cm bed heights, respectively, were measured into the column. Fluidization and bypass flow of the system were retarded by good packing of the adsorbent. Influent flow rate of 2.7, 4.2 and 5.7 mL/min in an upward direction with the aid of peristaltic pump (Master-flex, Cole-Parmer Instrument Co.) were used for 10, 15, and 20 mg/L initial concentrations of TZ. The effluent TZ concentration was measured at intervals at $\lambda_{max} = 425$ nm UV–Vis spectrophotometer. Experiments were continued until the column reached equilibrium concentration. All experiments were carried out under room temperature (25 ± 2 °C).

Fixed-bed column data analysis

Several bed parameters are important for the characterization of any adsorption process. They were determined for each column from the breakthrough curves using previously published calculation methods (Crhribi and Chlendi 2011; Casas et al. 2012; Chen et al. 2012).

The adsorption breakthrough profiles were obtained from C_t (mg/L) or C_t/C_o vs. V_t (mL) or t plots; where C_t is effluent concentration, C_o influent concentration, V_t volume of effluent treated and t is the service time. The treated effluent volume V_t is determined.as:

$$V_t = Q t_e \tag{2}$$

where Q (mL/min) and t_e are the influent flow rate and time of exhaustion. Fixed-bed capacity q_{total} (mg) at set influent
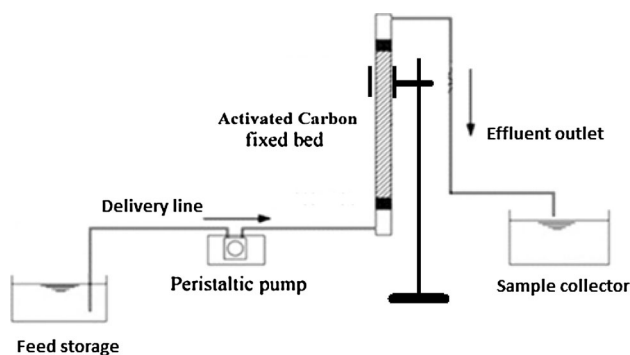
conditions (concentration and flow rate) is determined by computation of area under the plot from the integral of adsorbed concentrations expressed as; $C_{ad}(C_{ad} = C_o - C_t)$ mg/L for a given time t:

$$q_{total} = \frac{QA}{1000} = \frac{Q}{1000} \int_{t=0}^{t=t_{total}} C_{ad} dt \tag{3}$$

where t_{total}, is the total flow time, Q and A are the volumetric flow rate (mL/min) and the area under the breakthrough curve, respectively. The equilibrium uptake ($q_{eq(exp)}$) (mg/g) can be evaluated using Eq. (4) (Karunarathne and Amarasinghe 2013);

$$q_{eq(exp)} = \frac{q_{total}}{m} \tag{4}$$

where m (g) is the mass of adsorbent in the column.

Result and discussion

Adsorbent characterization

The nitrogen adsorption–desorption isotherms of activated carbon prepared from Apricot stone is depicted in Fig. 2, where the amount of N_2 adsorbed at 77 K is plotted against the relative pressure.

Figure 2 showed that the adsorption–desorption isotherm resemble a combination of types I and IV isotherms (in accordance with the International Union of Pure and Applied Chemistry (IUPAC) classification), which is corresponding to micro-mesoporous solid. The type IV isotherm usually originates from mesoporous solids. It describes a multilayer adsorption process where complete filling of the smallest capillaries has occurred. Whilst type I isotherm is typical of microporous solids where only monolayer adsorption occurs. In these micropores, filling
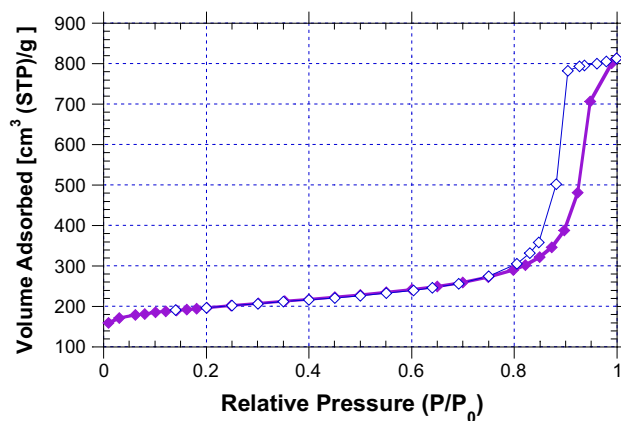

Fig. 1 Experimental setup for the fixed-bed adsorption process

Fig. 2 Adsorption profiles of N_2 at 77 K on the activated carbon prepared from apricot stone. *Open keys* indicate adsorption whilst *closed keys* indicate desorption

occurs significantly at relatively low partial pressure <0.1 p/p_o, the adsorption process being complete at $p/p_o \approx 0.5$. The main feature of such isotherm is the long plateau which is indicative of a relatively small amount of multi-layer adsorption on the open surface. On the other hands, the nitrogen uptake occurs mostly at ($p/p_o > 0.9$). This indicates that the meso- or macropore structure in the sample significantly developed. The isotherm is characterized by hysteresis loop, which appear in the multilayer rang of physical sorption isotherm. This kind of loop is generally associated with capillary condensation. It is well known that most mesoporous adsorbents give distinctive and reproducible hysteresis loops.

In Table 3 are given some textural parameters obtained from nitrogen adsorption isotherms at 77 K of the carbons samples prepared by H_3PO_4 chemical activation. The results revealed that activated carbons with well-developed porosity and high surface area can be manufactured from apricot stones. These superior properties could provide high concentration of active sites for adsorption of TZ dye to occur.

Knowledge on surface chemistry characteristics of the produced activated chars would give insight to its adsorption capability and behavior (Elsayed and Zalat 2015). FTIR analysis was conducted for qualitative characterization of surface functional groups of porous carbons activated by H_3PO_4. The IR spectrum of AC prepared by H_3PO_4 activation is shown in Fig. 3. The FTIR spectra show a number of significant peaks, indicating the complex structure of the chemical activated carbon sample. According to the spectrum, the appearance of bands at 3448.5–3421.5 cm^{-1} refers to (O–H) stretching vibrations in the hydroxyl, carboxylic or phenolic groups. The band appears at 2854.5 cm^{-1} can be assigned to C–H group stretching. The band appears at 1635.5 cm^{-1} can be assigned explained to the olefinic C=C stretching. In fact, the C=C stretching absorption frequently occurs at approximately nearby 1600 cm^{-1} for carbonaceous materials (Aygun et al. 2003), The band shift from 1600 cm^{-1} may be due to conjugation with another C=C bond, or a C=O bond. The band located at 1384.8 cm^{-1} could be attributed to C–H deformation vibration in alkenes that frequently occurs at approximately at 1381 cm^{-1}. The

Table 3 The characteristic pore properties of resulting activated carbon

	S_{BET}^a (m²/g) ±10	V_t^b (cm³/g) ±0.02	V_{mic}^c (cm³/g) ±0.02	V_{mes}^d (cm³/g) ±0.02	D_p^e (nm) ±0.02
Activated carbon (AC)	774	1.26	0.30	0.95	7.48

[a] Specific surface area determined from the BET equation

[b] Total pore volume, calculated from the amount of vapor adsorbed at a relative pressure of (0.99)

[c] Micropore volume determine by Horvath-Kawazoe model, calculated from the amount of nitrogen adsorbed at relative pressure (p/p_o) of 0.20

[d] Mesopore volume, calculated by subtracting the amount adsorbed at a relative pressure of 0.2 from that adsorbed at relative pressure of 0.99

[e] Mean pore diameter, calculated from (4 V_t/S_{BET}). Note; the number of significant figures quoted in the table an indication of precision

Fig. 3 IR spectrum of prepared activated carbon sample
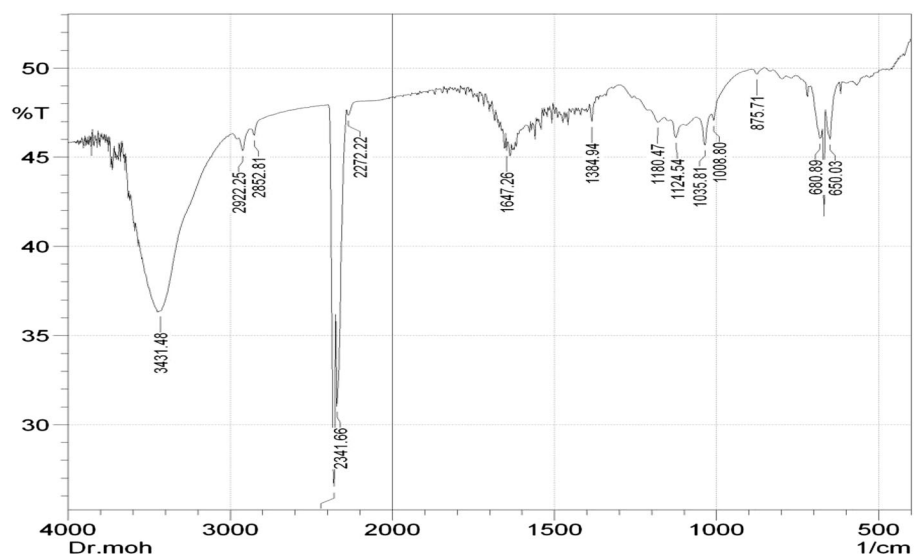
appearance of bands between 1033.8 and 1037.6 cm^{-1} could be assigned to C–O stretching vibrations in phenolic and carboxylic groups. The bands at 680–700 cm^{-1} may refer to C–H vibration. The data mentioned above show the presence of phenolic, carboxylic and hydroxylic groups, which may be responsible for the potential adsorption of TZ dye onto the prepared AC sample (Baraka 2012).

Effect of contact time and initial dye concentration on adsorption equilibrium

Figure 4 shows the adsorption capacity vs. the adsorption time at various initial TZ concentrations at 25 °C. It indicated that the contact time needed for TZ solutions with initial concentrations of 25–100 mg/L to reach equilibrium was 120 min. As can be seen from Fig. 3, the amount of TZ adsorbed onto the activated carbon increased with time and, at some point in time, it reached a constant value beyond which no more TZ dye was further removed from the solution. At this point, the amount of the TZ dye desorbing from the activated carbon was in a state of equilibrium with the amount of the TZ dye being adsorbed onto the activated carbon. The amount of dye adsorbed at the equilibrium time reflects the maximum adsorption capacity of the adsorbent under those operating conditions. In this study, the adsorption capacity at equilibrium (q_e) increased from 22.6 to 76 mg/g with an increase in the initial dye concentrations from 25 to 100 mg/L. The effect of the initial dye concentration depends on the immediate relation between the dye concentration and the available binding sites on an adsorbent surface (Gautam et al. 2014b).

Generally, the adsorption capacity of activated carbon samples and the percentage of dye removal decrease with an increase in initial dye concentration, which may be due to the saturation of adsorption sites on the adsorbent surface. At low initial dye concentration, there will be unoccupied active sites on the activated carbon surface,
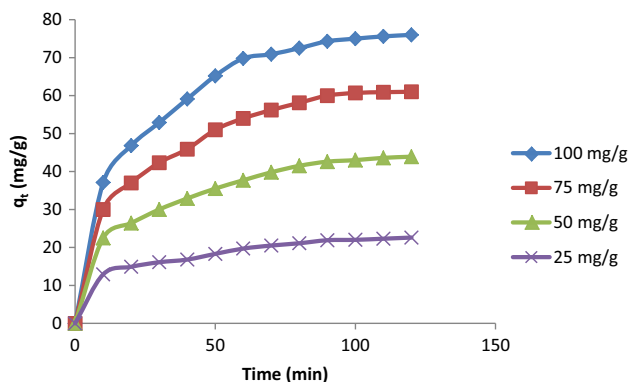
and when the initial dye concentration increases, the active sites required for adsorption of the dye molecules will occupy and disappear (Gautam et al. 2013). However, the increase in the initial dye concentration leading to the high driving force for mass causes an increase in the loading capacity of the adsorbent. In other words, the number of dye molecules in the solution will be higher than active sites available on the adsorbent surface for higher initial dye concentrations. In contrast, at the case of lower initial dye concentrations, the ratio of initial number of dye molecules in the solution to the available adsorption active sites on the surface of the adsorbent is low and subsequently the fractional adsorption becomes independent of initial concentration (Gautam et al. 2014a).

Effect of temperature on adsorption equilibrium and thermodynamic parameters

Figure 5 shows the adsorption equilibrium vs. temperature at initial TZ concentrations 100 ppm. It is shown that the adsorption capacity increases with temperature, indicating an endothermic process. It had been investigated from the experiment that with the rise of temperature from 288 to 303 K the amount of dye uptake increases from 57 to 80 mg/g. As the rate of diffusion of the dye molecules is a temperature controlled process, variation in temperature alters the equilibrium capacity of the adsorbent for a particular adsorbate. In the present study, an increases of the adsorption temperature leads to fast diffusion of dye molecules across the external boundary layer and internal pore structure of the adsorbent particles. This may be due to less resistance offered by viscous forces in the solutio. In addition, in some cases the solubility of the dye molecules is affected with the increase of the temperature which finally has a significant impact on the removal efficiency.

Fig. 4 Adsorption capacity vs. adsorption time at various initial TZ concentrations at 25 °C
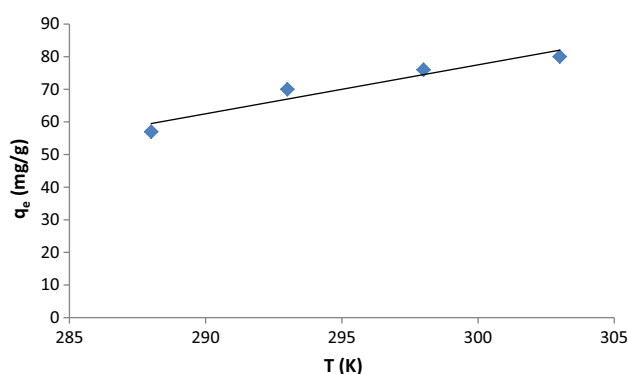

Fig. 5 Effect of temperature on adsorption equilibrium at initial TZ concentrations (100 ppm)

The thermodynamics of the adsorption process were studied at three different temperatures in a thermostated incubator. Thermodynamic parameters such as the Gibbs free energy change (ΔG), enthalpy changes (ΔH) and entropy change (ΔS) can be used for the characterization of temperature effect on the adsorption process. These parameters were calculated using the following equations:

$$\Delta G = -RTLnK_L \text{ (Gibbs equation)} \quad (5)$$

$$LnK_L = -\frac{\Delta H}{RT} + \frac{\Delta S}{R} \text{ (Vant' Hoff equation)} \quad (6)$$

where $K_L = \frac{q_e}{C_e}$, R is the molar gas constant (8.314 J/mol K) and T is the absolute temperature. K_L is the equilibrium constant obtained for each temperature from the Langmuir model. ΔH and ΔS were obtained from the slopes and intercepts of the linear plots of In K_L against $1/T$ (Figure not shown). The values of the thermodynamic parameters are given in Table 4.

sitive value of (ΔH) 78.1(K J mol^{-1}) revealed that adsorption efficiency increased with an increase in the adsorption temperature; this implies that each TZ molecule had to displace more than one water molecule from the adsorbent surface before it is adsorbed. Generally, most of the adsorption studies substantiate the assumption that the adsorption of dye on the active carbon surface is endothermic. Significantly, these high values of (ΔH) indicate a strong chemical interaction between the active carbon and TZ dye. The negative value of ΔG reflects the feasibility and spontaneity of the adsorption process. In addition, the value of ΔS (285 J mol^{-1} k^{-1}) had been expected to be so large which indicated an increase of entropy as a result of adsorption process (Gautam et al. 2013). This can be explained as that, before adsorption occurs, the dyes ions near the active carbon boundary were in ordered form than in the subsequent adsorbed state and the ratio of free dye ions to the captured dye ions with the active carbon will be higher than in the adsorbed state. As a result of adsorption, there will be an increased randomness at solid–liquid interface and the distribution of translational and rotational energy will increase, producing a positive entropy value. In the present study, at high operating temperature, adsorption is likely to occur spontaneously because $\Delta H > 0$ and $\Delta S > 0$.

Fixed-bed adsorption column study

Effect of bed height on breakthrough curve

An effect of bed height on the adsorption of TZ by activated carbon samples is shown in Fig. 6. In this experiment the bed heights were 8, 10 and 12 cm with fixed flow rate of 2.7 mL/min, 15 mg/L TZ concentration and pH = 6.8.

Increase in bed height of adsorption columns leads to longer breakthrough point as well as the exhaustion time of adsorbent. This is due to increase in the amount of adsorbent in the column which leads to increase in surface area (Khoo et al. 2012). The shape and gradient of the breakthrough curves were slightly different for different bed height.

It was also observed that, the sorption capacity and breakthrough time increased with an increase in the bed height as shown in Table 5. This increase can be attributed to sufficient residence time of TZ dye in the column adsorption region which provided sufficient time for diffusion or interaction of the dye molecules with the adsorbent. An increase in adsorption capacity of TZ from 1.61 to 2.41 mg/g was recorded.

The BDST model proposed by Bohart and Adams offer the simplest approach and most rapid prediction of column adsorption performance (Vaňková et al. 2010). The model gives a linear relationship between the time required to
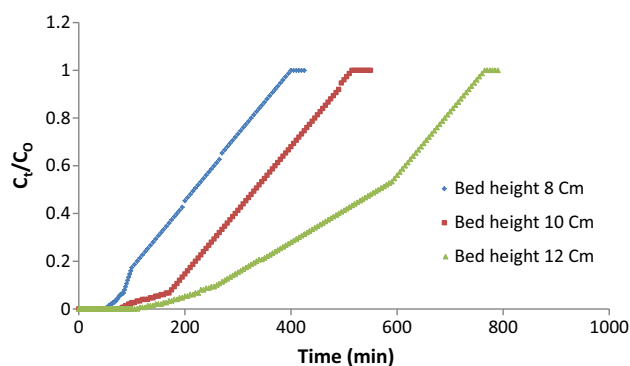

Fig. 6 Effect of bed height on adsorption of TZ by activated carbon (flow rate of 2.7 mL/min, Initial TZ concentration of 15 mg/L, and temperature of 25 °C)

Table 4 Values of thermodynamic parameters for the removal of Tartrazine onto AC

Temperature (K)	ΔG (K J mol^{-1})	ΔH (K J mol^{-1})	ΔS (mol^{-1}k^{-1})
288	−4.49	78.4	285
298	−6.16		
303	−9.8		

Table 5 Experimental constants of BDST model for TZ adsorption onto activated carbon (TZ concentration = 15 ppm, pH = 6.8 and flow rate = 2.7 mL/min)

Bed depth	q_e (mg/g)	t_b (min)	t_e (min)	R^2
8 cm	1.61	52	425	0.99
10 cm	1.78	82	550	
12 cm	2.41	115	790	

reach the desired breakthrough concentration and the bed height. The equation can be expressed as follows:

$$t = \frac{N_o Z}{C_o Q} - \frac{1}{K_a C_o} \ln\left(\frac{C_o}{C_t} - 1\right) \quad (4)$$

where C_t is the breakthrough dye concentration (mg/L), C_O is influent or initial solute concentration (mg/L), N_0 the sorption capacity of bed (mg/L), Q the linear velocity (mL/min), Z is the depth of adsorbent bed and K_a is the rate constant (L/mg min).

The plot of service time against bed height at a flow rate of 2.7 mL/min was linear indicating the validity of BDST model (Fig. 7). The results of different bed height showed the validity of BDST model to study adsorption of TZ with the regression coefficient (R^2) of 0.99, (Table 4). The value of adsorption capacity of the bed per unit of bed volume, N_o and the rate constant, K_a were computed from the slope and intercept of BDST plot assuming initial concentration, C_o and the linear velocity, as constant. The rate constant, K_a is a measure of the rate transfer of dye solution from the fluid phase to the solid phase. For TZ adsorption the values of N_o and K_a were 637.8 mg/L and 0.002 L/mg h, The parameters obtained from BDST plot can be used to scale-up the process (Walker and Weatherley 1997).

A higher bed height indicates a larger amount of binding sites available. Similar observations also have been reported by several researchers (Unuabonah et al. 2010; Mulgundmath et al. 2012; Noreen et al. 2013). The longer exhaustion time (t_e, the time that the effluents reach the influent concentration) was observed by increasing the bed height from 8 to 12 cm. The exhaustion time also increased from 425 to 790 min for TZ adsorption. After breakthrough time (t_b, the time that the effluents concentration start to be detected), the concentration of effluent of dyes TZ rapidly increases.

Validity of kinetic models of fixed-bed column adsorption

Dynamic adsorption is a complex process and its performance is controlled by many variables (Chen et al. 2012).
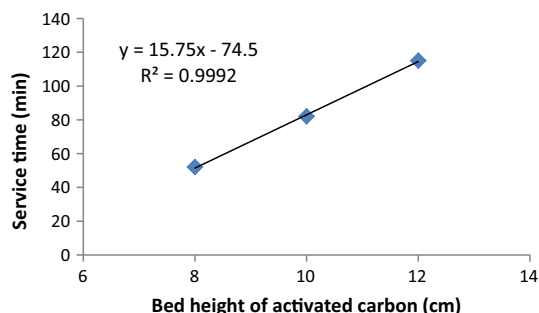
In conducting packed-bed sorption experiments, normally the results are presented in terms of concentration time profile or breakthrough curve. The process of calculation is complicated and time consuming. Prediction of the adsorption rate and the maximum sorption bed capacity can be determined by applying certain mathematical models (Vaňková et al. 2010; Unuabonah et al. 2010).

Thomas model is widely used in predicting column performance modeling. Its derivation assume Langmuir isotherm for equilibrium, plug flow behavior in the bed and second-order reversible reaction kinetics. This model is suitable for studying fixed-bed adsorption processes where the internal and external diffusion limitations are negligible. The linearized form of Thomas model can be expressed as follows (Sidiras et al. 2011):

$$\ln\left(\frac{C_0}{C_t} - 1\right) = \frac{k_{Th} q_e W}{Q} - k_{Th} C_0(t) \quad (5)$$

where q_e (mg/g) is the equilibrium dye uptake per g of the adsorbent; k_{Th} (mL/min mg) is the Thomas rate constant; C_o (mg/L) is the inlet concentration; C_t (mg/L) is the outlet concentration at time t; Q (mL/min) the flow rate; W (g) the mass of adsorbent, and (t) stands for flow time. The value of C_0/C_t is the ratio of inlet and outlet dye concentrations. A linear plot of $\ln[(C_o/C_t) - 1]$ against time (t) was employed to determine values of k_{Th} and q_e from the intercept and slope of the plot as shown in Figs. 8 and 9 for TZ adsorption.

The Thomas model gave a good fit of experimental data with high coefficient of determination, R^2 is greater than 0.92. The values of Thomas model show that the maximum adsorption capacities increases with increasing initial concentrations. However, the maximum adsorption capacities decrease with increases of flow rate. Table 6 shows the coefficient of determination values were varied from 0.92 to 0.98 with relative errors (RE) variation from 2.8 to
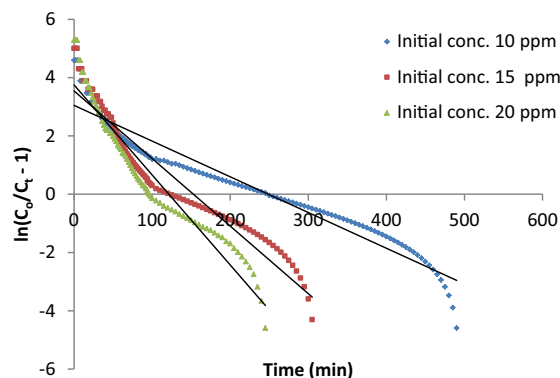
Fig. 7 BDST model plot for TZ adsorption onto activated carbon bed (C_o = 15 mg/L, pH = 7, flow rate = 2.7 mL/min.)

Fig. 8 Thomas model for adsorption of TZ on activated carbon at different initial concentration (flow rate of 2.7 mL/min, bed height of 10 cm, temperature of 25 °C)
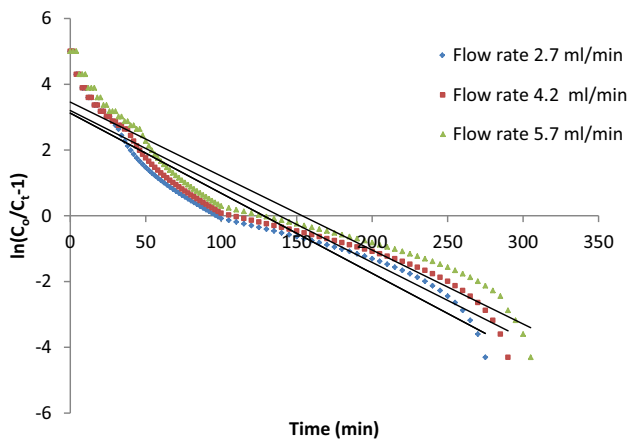
Fig. 9 Thomas model for adsorption of TZ on activated carbon at different flow rates (bed height of 10 cm, Initial TZ concentration of 15 mg/L, and temperature of 25 °C)

8.9 which indicate a good agreement between the experimental data and the column data generated using the Thomas model. The rate constant, K_{Th} is observed to increase and decrease with the same pattern with q_e (mg/g) (the calculated equilibrium dye uptake per gram of the adsorbent) (Futalan et al. 2011).

Bohart–Adams model which describes the initial part of a breakthrough profile is assumed to have rectangular shape isotherm. The model equation can be expressed as:

$$\ln\left(\frac{C_t}{C_0}\right) = k_{AB}C_0(t) - \frac{k_{AB}N_0Z}{L} \tag{6}$$

where C_0 and C_t are the initial and breakthrough concentrations (mg/L), N_0 is fixed-bed sorption capacity per unit volume (mg/mL), k_{AB} (mL/mg min) is Bohart–Adams model's constant, Z is the bed height, L (mL/min) is the linear or superficial velocity and t_b is the breakthrough time. The model's parameters are obtained from the intercept and slope of a linear plot of ln $[(C_t/C_0)]$ against t_b as shown in Figs. 10 and 11 for TZ adsorption.

Linear regression results (Table 7) shown that adsorption capacity of the adsorbent (N_0) and kinetic constant of the model (k_{AB}) increased with increasing initial dye concentration. However, because of more saturation of active carbon sites, adsorption capacity of the adsorbent (N_0) decreased with increasing flow rate. In addition, kinetic constant of the model (k_{AB}) decrease with increasing flow rate. The lower R^2 values relative to the other model can be interpreted that the Adams–Bohart model is not as appropriate a predictor for the breakthrough curve (Rozada et al. 2003).

Adsorption performance of prepared activated carbon

The adsorption capacities of tartrazine over a variety of adsorbents are compared and reported in Table 8. The adsorption capacity of apricot stones based activated carbon prepared in this study was found to be larger than adsorption capacity accounted by several researcher from batch studies. Therefore, the activated carbon prepared in this work could be used as an effective adsorbent for removing azo-dye from aqueous solutions. However, the TZ adsorption capacity obtained from the column experiments was lower than the values obtained from the batch experiments for the same initial dye concentrations used. This might be due to the insufficient contact time between the dye ions in the solution and the adsorbent in the column. The difference between the batch and continuous capacity could also be attributed to the channeling of the flowing stream. Besides, the effective surface area of the activated carbons adsorbent packed in the column was lower than that in the batch process. Therefore, the performance of the activated carbon bed could be enhanced by applying a lower solution flow rate and/or using a higher bed height.

Table 6 Thomas model parameter of TZ adsorption on AC

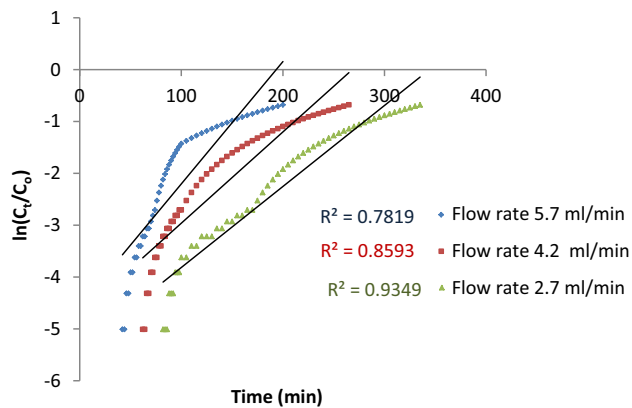| Inlet conc. (mg/L)	Bed height, H	Flow rate (mL/min)	Parameters				
			k_{Th} (mL/min mg)	q_e (mg/g)	R^2	$q_{e(exp)}$	RE
Effect of initial concentration							
10	10	2.7	1.05	1.70	0.934	1.56	8.97
15	10	2.7	1.12	1.86	0.973	1.78	4.49
20	10	2.7	1.81	1.98	0.963	1.84	7.61
Effect of flow rate							
15	10	2.7	1.23	2.53	0.970	2.46	2.80
15	10	4.2	1.11	2.35	0.948	2.28	3.07
15	10	5.7	1.06	1.88	0.968	1.76	6.81

Fig. 10 Adam's–Bohart model for adsorption of TZ onto activated carbon at different flow rate (bed height of 10 cm, Initial TZ concentration of 15 mg/L, and temperature of 25 °C)
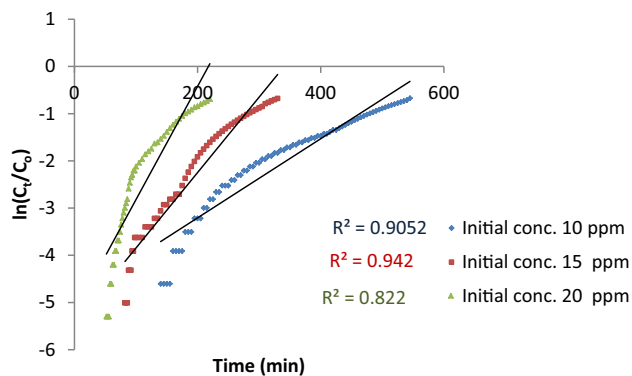

Fig. 11 Adam's–Bohart model for adsorption of TZ on activated carbon at different initial concentration (flow rate of 2.7 mL/min, bed height of 10 cm, temperature of 25 °C)

Table 7 Adam-Bohart model parameter of TZ adsorption on AC

Dye inlet conc. (mg/L)	Bed height, H	Flow rate (mL/min)	Parameters		
			k_{AB} (mL/ mg. min)	N_0 (mg/ mL)	R^2
Effect of initial concentration					
10	10	2.7	0.50	1.57	0.90
15	10	2.7	0.67	1.79	0.94
20	10	2.7	0.81	2.19	0.82
Effect of flow rate					
15	10	2.7	0.62	2.83	0.93
15	10	4.2	0.41	2.57	0.86
15	10	5.7	0.30	1.78	0.78

Table 8 Comparison of the adsorption capacity of Apricot stone-based activated carbon with various adsorbents

Adsorbent	Maximum adsorption capacity (mg/g)	References
Jute processing wastes	22.47	Banerjee and Dastidar (2005)
Chitin	30	Dotto et al. (2012)
Polyaniline nano layer composite	2.47	Ansari et al. (2011)
Bottom ash	12.6	Mittal et al. (2006)
Deoiled soya	24.6	Mittal et al. (2006)
Amberlite IRA-900	49.88	Wawrzkiewicz and Hubicki (2009)
Amberlite IRA-910	49.96	Wawrzkiewicz and Hubicki (2009)
Commercial activated carbon	4.48	Jibril et al. (2013)
Sawdust	4.71	
Apricot stone-based activated carbon	76	This study

adsorption–desorption isotherm was a combination of types I and IV isotherms, which is corresponding to micro-mesoporous solid. Studies on continuous adsorption using a series of column experiments revealed that activated carbon prepared from apricot stones by H_3PO_4 activation has high ability to remove Tartrazine dye from aqueous solutions. The continuous adsorption system represented by the breakthrough curves was dependent on the initial dye concentration, bed height and the solution flow rate used. The results of different bed height showed the validity of BDST model to study adsorption of TZ with the regression coefficient (R^2) of 0.99. Comparison of Thomas and Adams–Bohart kinetic models with experimental data was performed and model parameters were determined by linear regression analysis for TZ adsorption under various operating conditions. The experimental data fit well with Thomas, but the Adams–Bohart model predicted poor performance of fixed-bed column.

Conclusions

Activated carbon with surface areas 774 m^2/g and 1.26 cm^3/g pore volume can be produced from apricot stone by utilizing H_3PO_4 as an activating agent. The N_2

References

Aguilar F, Charrondiere UR, Dusemund B, Galtier P, Gilbert J, Gott DM, Grilli S, Guertler R, Koenig J (2009) Scientific Opinion on

the re-evaluation tartrazine (E 102). Eur Food Safety Auth 7(11):1331

Ahmad A, Hameed B (2010) Fixed-bed adsorption of reactive azo dye onto granular activated carbon prepared from waste. J Hazard Mater 175(1):298–303

Algidsawi AJK (2011) A study of ability of adsorption of some dyes on activated carbon from date' stones. Aust J Basic Appl Sci 5(11):1397–1403

Annadurai GJR, Lee DJ (2002) Adsorption of heavy metals from water using banana and orange peels. Water Sci Technol 47(1):185–190

Annadurai GJRS, Lee DJ, Juang Ruey-Shin, Lee Duu-Jong (2002) Use of cellulose-based wastes for adsorption of dyes from aqueous solutions. J Hazard Mater B92:263–274

Ansari R, Banimahd Keivani M, Fallah Delavar A (2011) Application of polyaniline nanolayer composite for removal of tartrazine dye from aqueous solutions. J Polym Res 18(6):1931–1939. doi:10.1007/s10965-011-9600-z

Aygun A, Karakas S, Duman I (2003) Production of granular activated carbon from fruit stones and nutshells and evaluation of their physical, chemical and adsorption properties. Micropor Mesopor Mater 66:189–195

Banerjee S, Dastidar M (2005) Use of jute processing wastes for treatment of wastewater contaminated with dye and other organics. Bioresour Technol 96(17):1919–1928

Baraka A (2012) Adsorptive removal of tartrazine and methylene blue from wastewater using melamine-formaldehydetartaric acid resin (and a discussion about pseudo second order model). Desalination Water Treat 44:128–141

Casas N, Schell J, Pini R, Mazzotti M (2012) Fixed bed adsorption of CO_2/H_2 mixtures on activated carbon: experiments and modeling. Adsorption 18(2):143–161

Chen S, Yue Q, Gao B, Li Q, Xu X, Fu K (2012) Adsorption of hexavalent chromium from aqueous solution by modified corn stalk: a fixed-bed column study. Bioresour Technol 113:114–120

Crhribi A, Chlendi M (2011) Modeling of fixed bed adsorption: application to the adsorption of an organic dye. Asian J Textile 1:161–171

Deng H, Yang L, Tao G, Dai J (2009) Preparation and characterization of activated carbon from cotton stalk by microwave assisted chemical activation—application in methylene blue adsorption from aqueous solution. J Hazard Mater 166(2–3):1514–1521. doi:10.1016/j.jhazmat.2008.12.080

Dotto GL, Vieira MLG, Pinto LAA (2012) Kinetics and mechanism of tartrazine adsorption onto chitin and chitosan. Ind Eng Chem Res 51(19):6862–6868. doi:10.1021/ie2030757

Dutta M, Basu J (2014) Fixed-bed column study for the adsorptive removal of acid fuchsin using carbon–alumina composite pellet. Int J Environ Sci Technol 11(1):87–96

Elsayed M, Zalat O (2015) Factor affecting microwave assisted preparation of activated carbon from local raw materials. Int Lett Chem Phys Astron 8(1):15

Futalan CM, Kan C-C, Dalida ML, Pascua C, Wan M-W (2011) Fixed-bed column studies on the removal of copper using chitosan immobilized on bentonite. Carbohydr Polym 83(2):697–704

Gautam RK, Mudhoo A, Chattopadhyaya MC (2013) Kinetic, equilibrium, thermodynamic studies and spectroscopic analysis of Alizarin Red S removal by mustard husk. J Environ Chem Eng 1(4):1283–1291

Gautam RK, Gautam PK, Chattopadhyaya M, Pandey J (2014a) Adsorption of alizarin red s onto biosorbent of lantana camara: kinetic, equilibrium modeling and thermodynamic studies. Proc Natl Acad Sci India Sect A Phys Sci 84(4):495–504

Gautam RK, Mudhoo A, Lofrano G, Chattopadhyaya MC (2014b) Biomass-derived biosorbents for metal ions sequestration: adsorbent modification and activation methods and adsorbent regeneration. J Environ Chem Eng 2(1):239–259

Gautam RK, Gautam PK, Banerjee S, Rawat V, Soni S, Sharma SK, Chattopadhyaya MC (2015a) Removal of tartrazine by activated carbon biosorbents of Lantana camara: kinetics, equilibrium modeling and spectroscopic analysis. J Environ Chem Eng 3(1):79–88

Gautam RK, Rawat V, Banerjee S, Sanroman MA, Soni S, Singh SK, Chattopadhyaya MC (2015b) Synthesis of bimetallic Fe–Zn nanoparticles and its application towards adsorptive removal of carcinogenic dye malachite green and Congo red in water. J Mol Liq 212:227–236

Grégorio Crini P-MB (2010) Sorption processes and pollution: Conventional and non-conventional sorbents for pollutant removal from wastemasters. Presses Univ, Franche-Comté

Gupta V, Gupta B, Rastogi A, Agarwal S, Nayak A (2011) A comparative investigation on adsorption performances of mesoporous activated carbon prepared from waste rubber tire and activated carbon for a hazardous azo dye—acid blue 113. J Hazard Mater 186(1):891–901

Gurses AKS, Dogar C, Bayrak R, Acikyildiz M, Yalcin M (2004) Determination of adsorptive properties of clay/water system: methylene blue sorption. J Colloid Interface Sci 269(2):310–314

Jibril M, Noraini J, Poh LS, Evuti AM (2013) Removal of colour from waste water using coconut shell activated carbon (CSAC) and commercial activated carbon (CAC). Jurnal Teknologi 60(1):15–19

Kadirvelu K, Kavipriya M, Karthika C, Radhika M, Vennilamani N, Pattabhi S (2003) Utilization of various agricultural wastes for activated carbon preparation and application for the aqueous solutions. Bio Resour Technol 87:129–132

Karunarathne H, Amarasinghe B (2013) Fixed bed adsorption column studies for the removal of aqueous phenol from activated carbon prepared from sugarcane bagass. Energy Proc 34:83–90

Khoo E-C, Ong S-T, Ha S-T (2012) Removal of basic dyes from aqueous environment in single and binary systems by sugarcane bagasse in a fixed-bed column. Desalination Water Treat 37(1–3):215–222

Klán P, Vavrik M (2006) Non-catalytic remediation of aqueous solutions by microwave-assisted photolysis in the presence of H_2O_2. J Photochem Photobiol A 177(1):24–33. doi:10.1016/j.jphotochem.2005.05.008

Mittal A, Mittal J, Kurup L (2006) Adsorption isotherms, kinetics and column operations for the removal of hazardous dye, tartrazine from aqueous solutions using waste materials—bottom ash and de-oiled soya, as adsorbents. J Hazard Mater 136(3):567–578. doi:10.1016/j.jhazmat.2005.12.037

Mulgundmath V, Jones R, Tezel F, Thibault J (2012) Fixed bed adsorption for the removal of carbon dioxide from nitrogen: breakthrough behaviour and modelling for heat and mass transfer. Sep Purif Technol 85:17–27

Namasivayam CRR, Suba S (2001) Uptake of dyes by a promising locally available agricultural solid waste: coir pith. J Waste Manag 2:381–387

Noreen S, Bhatti HN, Nausheen S, Sadaf S, Ashfaq M (2013) Batch and fixed bed adsorption study for the removal of drimarine black CL-B dye from aqueous solution using a lignocellulosic waste: a cost affective adsorbent. Ind Crops Prod 50:568–579

Robinson T, McMullan G, Marchant R, Nigam P (2001) Remediation of dyes in textiles effluent: a critical review on current treatment technologies with a proposed alternative. Bioresour Technol 77:247–255

Robinson T, Chandran B, Nigam P (2002) Studies on desorption of individual textile dyes and a synthetic dye effluent from dye adsorbed agricultural residues using solvents. Bioresour Technol 58:217–227

Rozada F, Calvo L, García A, Martín-Villacorta J, Otero M (2003) Dye adsorption by sewage sludge-based activated carbons in batch and fixed-bed systems. Bioresour Technol 87(3):221–230

Santhy K, Selvapathy P (2006) Removal of reactive dyes from wastewater by adsorption on coir pith activated carbon. Bioresour Technol 97(11):1329–1336

Sidiras D, Batzias F, Schroeder E, Ranjan R, Tsapatsis M (2011) Dye adsorption on autohydrolyzed pine sawdust in batch and fixed-bed systems. Chem Eng J 171(3):883–896

Unuabonah EI, Olu-Owolabi BI, Fasuyi EI, Adebowale KO (2010) Modeling of fixed-bed column studies for the adsorption of cadmium onto novel polymer–clay composite adsorbent. J Hazard Mater 179(1):415–423

Vaňková K, Ačai P, Polakovič M (2010) Modelling of fixed-bed adsorption of mono-, di-, and fructooligosaccharides on a cation-exchange resin. Biochem Eng J 49(1):84–88

Walker G, Weatherley L (1997) Adsorption of acid dyes on to granular activated carbon in fixed beds. Water Res 31(8):2093–2101

Wawrzkiewicz M, Hubicki Z (2009) Removal of tartrazine from aqueous solutions by strongly basic polystyrene anion exchange resins. J Hazard Mater 164(2–3):502–509. doi:10.1016/j.jhazmat.2008.08.021

Yavuz Ö, Aydin AH (2006) Removal of direct dyes from aqueous solution using various adsorbents. Pol J Environ Stud 15(1):155–161